

# Multi-Dimensional Simulations of Radiative Transfer in Aspherical Core-Collapse Supernovae

Masaomi Tanaka<sup>\*</sup>, Keiichi Maeda<sup>†,\*\*</sup>, Paolo A. Mazzali<sup>\*\*,‡</sup> and Ken'ichi Nomoto<sup>†,\*</sup>

<sup>\*</sup>*Department of Astronomy, Graduate School of Science, University of Tokyo, Tokyo, Japan;*  
*mtanaka@astron.s.u-tokyo.ac.jp*

<sup>†</sup>*Institute for the Physics and Mathematics of the Universe, University of Tokyo, Kashiwa, Japan*

<sup>\*\*</sup>*Max-Planck-Institut für Astrophysik, Garching bei München, Germany*

<sup>‡</sup>*Istituto Nazionale di Astrofisica, OATs, Trieste, Italy*

## Abstract.

We study optical radiation of aspherical supernovae (SNe) and present an approach to verify the asphericity of SNe with optical observations of extragalactic SNe. For this purpose, we have developed a multi-dimensional Monte-Carlo radiative transfer code, SAMURAI (SupernovA Multi-dimensional RAdIative transfer code). The code can compute the optical light curve and spectra both at early phases ( $\lesssim 40$  days after the explosion) and late phases ( $\sim 1$  year after the explosion), based on hydrodynamic and nucleosynthetic models. We show that all the optical observations of SN 1998bw (associated with GRB 980425) are consistent with polar-viewed radiation of the aspherical explosion model with kinetic energy  $20 \times 10^{51}$  ergs. Properties of off-axis hypernovae are also discussed briefly.

**Keywords:** supernovae; gamma-ray bursts; radiative transfer; nucleosynthesis

**PACS:** 97.60.Bw; 97.10.Ex; 26.30.-k

## INTRODUCTION

Although the explosion mechanism of core-collapse supernovae (SNe) is not well understood, there is several observational evidence of non-spherical explosion, obtained by the imaging of *very* nearby SNe, e.g., SN 1987A [1] and Galactic supernova remnants [2]. Even when the imaging is not possible, the detection of polarization from extragalactic SNe [3, 4, 5] suggests that SNe are not spherical. In addition to these studies, spectroscopy of SNe can also give clues of the structure of SN explosion. For example, emission line profiles in the late time spectra ( $t \gtrsim 1$  year, where  $t$  is the time after the explosion) reveals the asphericity of the explosion [6].

It is well established that a special class of Type Ic SNe<sup>1</sup> are associated with the long gamma-ray bursts (GRBs, see [8] and references therein). This class of SNe is thought to be highly energetic, so called hypernovae (here defined as SNe with ejecta kinetic energy  $E_{51} = E_K/10^{51}$  ergs  $> 10$ ; e.g., [9]). The asphericity of hypernovae is of great

---

<sup>1</sup> SNe that do not show H, He, and strong Si absorption in the early time spectra ( $t \lesssim 40$  days) are classified as Type Ic [7].

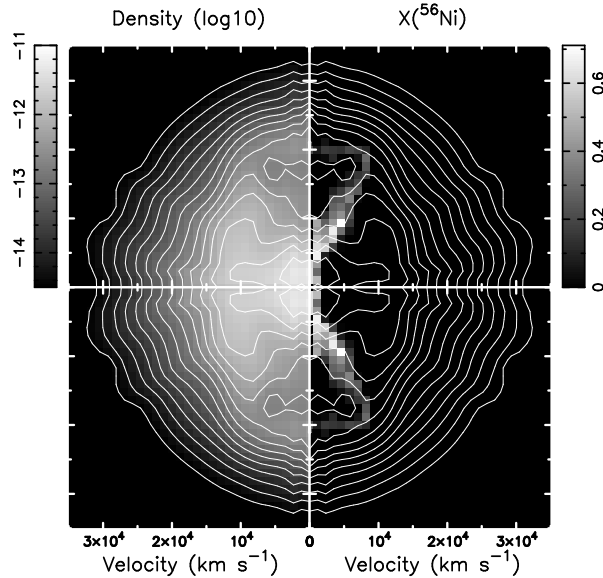


**FIGURE 1.** Aspherical explosion model A20 with the kinetic energy  $E_{51} = E_K/10^{51}\text{ergs} = 20$ . *Left:* Density distribution ( $\log g \text{ cm}^{-3}$ ) at  $t=10$  days. The contour also shows the density. *Right:* Mass fraction of  $^{56}\text{Ni}$ . The velocity can be used as spatial coordinate thanks to the homologous expansion ( $r \propto v$ ).

interest related to the nature of GRBs.

Since GRBs are induced by relativistic jets, hypernovae are also thought to be aspherical. However, the large kinetic energy of hypernovae is estimated by the analysis under the spherical symmetry. No realistic multi-dimensional explosion models have been verified against the observed early phase spectra.

To study the multi-dimensional nature of the SN explosion through the various observational facts, radiative transfer calculations are required to connect observables and hydrodynamics models. In this paper, radiative transfer in SN ejecta is solved with a multi-dimensional Monte-Carlo radiative transfer code, SAMURAI (Supernova Multi-dimensional RAdiative transfer code), based on hydrodynamic and nucleosynthetic models of hypernovae. The results are compared with observations of SN 1998bw, and implications for off-axis hypernovae are discussed.

## EXPLOSION MODELS

We use the results of multi-dimensional hydrodynamic and nucleosynthetic calculations for SN 1998bw [10] as input density and element distributions. Figure 1 shows the density structure and the distribution of  $^{56}\text{Ni}$ . Since the original models used a He star as a progenitor, we simply replace the abundance of the He layer with that of the C+O layer. In the hydrodynamic model, energy is deposited aspherically, with more energy in the jet direction (z-axis, defined as  $\theta = 0^\circ$ ). As a result,  $^{56}\text{Ni}$  is preferentially synthesized along this direction (right panel of Fig. 1). In this paper, an aspherical model with  $E_{51} = 20$  (A20) and a spherical model with  $E_{51} = 50$  (F50) are studied. They are constructed based on the models with  $E_{51} = 10$  [10, 11].

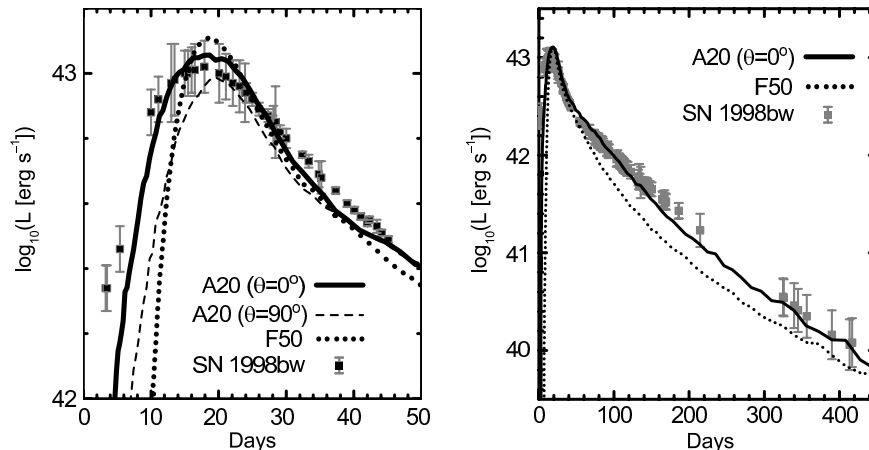


**FIGURE 2.** The LC of SN 1998bw (points) compared with the results of simulations. *Left:* The LCs at early phases. The LC of the polar-viewed model ( $\theta = 0^\circ$ ) rises earlier than that of the side-viewed model ( $\theta = 90^\circ$ ). *Right:* The LCs including late phases. The LC of the spherical model that explained early phase LC and spectra (F50) fades faster than the observed LC.

## THE NUMERICAL CODE

In order to study the detailed properties of the radiation from aspherical SNe, we have unified a Supernova MULTI-dimensional RADiative transfer code *SAMURAI*. *SAMURAI* is a combination of 3D codes adopting Monte-Carlo methods to compute the bolometric light curve (LC) [11, 12], and the spectra of SNe from early [13, 14] to late phases [15]<sup>2</sup>.

The early phase spectra are calculated as snapshots in the optically thin atmosphere, using the results of the LC simulation as initial conditions. A sharply defined photosphere is assumed as an inner boundary for simplicity. The position of the inner boundary in each direction is determined by averaging the positions of the last scattering photon packets (see Fig. 3 of Maeda et al. [11]). For the computation of ionization and excitation state in the atmosphere, the local physical process same as in the previous 1D code [22, 23]. Line scattering under the Sobolev approximation and electron scattering are taken into account. For line scattering, the effect of photon branching is included as in Lucy [24]. In the simulations, 16 elements are included, i.e., H, He, C, N, O, Na, Mg, Si, S, Ti, Cr, Ca, Ti, Fe, Co and Ni.

## LIGHT CURVES

Maeda et al. [11] computed bolometric LCs in 3D space. A common problem in hypernova LCs is that a spherical model reproducing the LC and spectra at early phases ( $E_{51} = 50$  for SN 1998bw) declines more rapidly than the observed LC at  $t \gtrsim 100$  days [25, 26] (see model F50 in the right panel of Fig. 2). This problem can be solved by

<sup>2</sup> See also [16, 17, 18, 19, 20, 21] for other multi-dimensional codes.

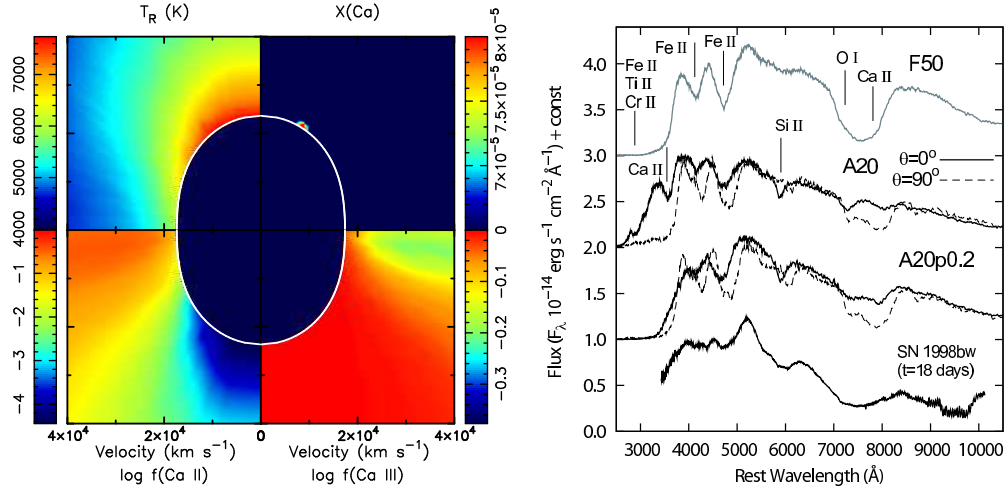


**FIGURE 3.** *Left:* Temperature structure (*upper left*), Ca mass fraction (*upper right*), ionization fraction of Ca II and Ca III (*lower left* and *lower right*, respectively) in the SN atmosphere at  $t = 20$  days. *Right:* The observed spectrum of SN 1998bw at  $t=18$  days compared with the synthetic spectra computed with model F50 (spherical), A20 (aspherical) and A20p0.2 (aspherical + mixing). For aspherical models, the solid and dashed lines show the spectra viewed from polar ( $\theta = 0^\circ$ ) and equatorial ( $\theta = 90^\circ$ ) direction, respectively. The synthetic spectra are scaled to match the observed spectra since the input luminosity is slightly brighter than the observation (Fig. 2, see Tanaka et al. [14] for details). The synthetic spectra are shifted by  $3.0, 2.0, 1.0 \times 10^{-14}$  from top to bottom.

aspherical models with a polar view. In aspherical models, even with a lower kinetic energy ( $E_{51} = 10 - 20$ , model A20 in Fig. 2) than in the spherical case ( $E_{51} = 50$ ), which allows sufficient trapping of  $\gamma$ -rays at late times, the rapid rise of the LC can be reproduced because of the extended  $^{56}\text{Ni}$  distribution [11].

## SPECTRA

The right panel of Figure 3 shows the synthetic spectra at  $t = 20$  days (around the maximum brightness) for models F50 and A20 compared with the observed spectrum of SN 1998bw. In model A20, all the absorption lines except for Si II  $\lambda 6355$  are stronger for larger  $\theta$ , i.e., for a side view. This is understood by the asphericity of the temperature structure in the SN atmosphere. As shown in the left panel of Figure 3, the temperature near the  $z$ -axis is higher than in the equatorial plane by  $\sim 2000$  K (*upper left*), tracing the aspherical distribution of  $^{56}\text{Ni}$ . This makes the ionization degree near the  $z$ -axis higher (*lower panels*). As a result, all species that have strong lines, i.e., O I, Si II, Ca II, Ti II, Cr II and Fe II, dominate near the equator but not near the  $z$ -axis.

The right panel of Figure 4 shows the synthetic spectra at  $t = 30$  days for models F50 and A20. The emergent spectra of the aspherical model are not significantly different for different viewing angles (Fig. 4). At this epoch, the temperature structure are still anisotropic, and consequently, the distribution of ionization fractions is also aspherical (see the left panel of Fig. 4). However, since nucleosynthesis occurs entirely near the polar direction in the model, and the photosphere at this epoch is located inside

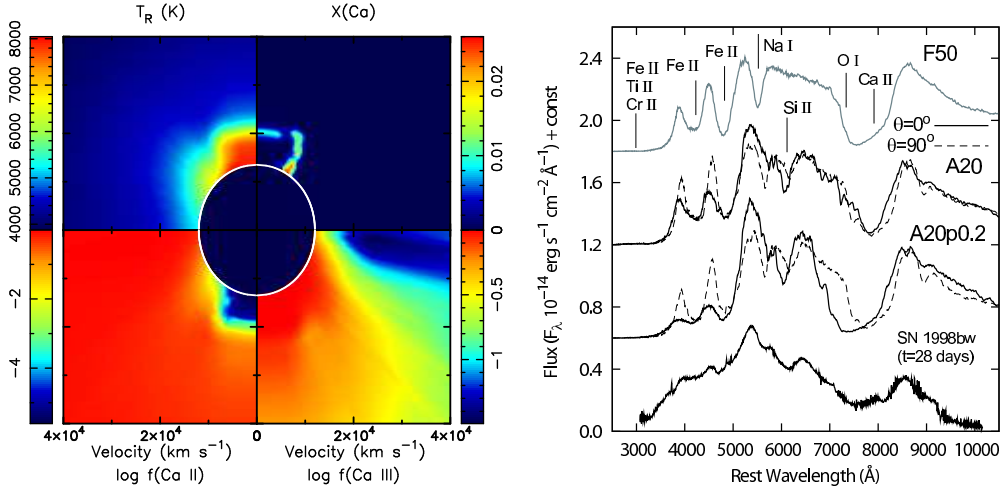


**FIGURE 4.** Same as Figure 3 but at  $t = 30$  days. The synthetic spectra are shifted by 1.8, 1.2,  $0.6 \times 10^{-14}$  from top to bottom.

the region where heavy elements are synthesized in the explosion, the suppression of important ions near the z-axis is compensated by the larger abundance of the heavy elements (see  $X(\text{Ca})$  in Fig. 4).

We compare the polar-viewed spectra of model A20 with the observed spectra of SN 1998bw. At  $t = 20$  days, the absorptions of O I, Ca II and Fe II/Fe III in the model are weaker than in SN 1998bw. At  $t = 30$  days, the Ca II and Fe II lines become strong, although the O I-Ca II absorption at  $7000 - 8000 \text{ \AA}$  is still narrower than in the observed spectrum. In the synthetic polar-viewed spectrum, the peaks around  $4000$  and  $4500 \text{ \AA}$  are partially suppressed by the high velocity absorption by the extended Fe near the jet, while they are strong in the side-viewed spectrum. The suppression of the peaks is similarly seen in the spectrum of SN 1998bw.

The strengths of the Ca II and Fe II lines at  $t = 20$  days can be increased if heavy elements synthesized in the explosion are mixed to outer layers. In SN explosions, Rayleigh - Taylor (R-T) instabilities are expected to occur (see Kifonidis et al. [27] for the case of Type Ic SNe), which could deliver the newly synthesized elements to higher velocities. In Figures 3 and 4, synthetic spectra of model A20p0.2 are also shown. In this model, 20% of synthesized material is assumed to be mixed to the outer layers. The agreement with the observed spectra becomes better especially at  $t = 20$  days.

## DISCUSSION

We have presented the detailed simulations of optical radiation with realistic jet-like hypernova models. The emergent LC and spectra are different for different viewing angles. The spectral properties are determined by the combination of aspherical abundances and anisotropic ionization states. Although the agreement of the spectra is far from perfect, the spectra of the model with mixing are in qualitative agreement with those of SN 1998bw.

The LC study shows that the kinetic energy of an aspherical model that explains SN 1998bw is  $E_{51} = 20$ , which is less than that of a well-fitting spherical model ( $E_{51} = 50$ ). The early phase spectra can also be explained by the model with  $E_{51} = 20$ . However, it should be noted that the higher kinetic energy than the canonical SNe ( $E_{51} \sim 1$ ) is still required.

The simulations enable us to predict the radiation from off-axis hypernovae. The LC viewed off-axis rises more slowly than that of on-axis, and its maximum brightness is fainter (Fig. 2). The spectra viewed off-axis show (1) a slightly lower absorption velocity, (2) stronger peaks around 4000 and 4500 Å (narrower absorption of Fe) and (3) a stronger Na I  $\lambda$ 5890 line. However, the spectra still show general appearance of “hypernovae” or “broad-line supernovae”. At later phases, off-axis hypernovae would show double-peaked [O I] emission profile [6, 15].

## ACKNOWLEDGMENTS

M.T. is supported through the JSPS (Japan Society for the Promotion of Science) Research Fellowship for Young Scientists.

## REFERENCES

1. Wang, L., et al. 2002, ApJ, 579, 671
2. Hwang, U., et al. 2004, ApJ, 615, L117
3. Wang, L., et al. 2001, ApJ, 550, 1030
4. Kawabata, K.S., et al. 2002, ApJ, 580, L39
5. Leonard, D.C., et al. 2006, Nature, 440, 505
6. Mazzali, P. A., et al. 2005, Science, 308, 1284
7. Filippenko, A.V., 1997, ARA&A, 35, 309
8. Woosley, S. E. & Bloom, J. S. 2006, ARA&A, 44, 507
9. Nomoto, K., et al. 2006, Nucl. Phys. A, 777, 424 (astro-ph/0605725)
10. Maeda, K., et al. 2002, ApJ, 565, 405
11. Maeda, K., Mazzali, P. A., & Nomoto, K. 2006a, ApJ, 645, 1331
12. Maeda, K. 2006, ApJ, 644, 385
13. Tanaka, M., et al. 2006, ApJ, 645, 470
14. Tanaka, M., et al. 2007, ApJ, 668, L19
15. Maeda, K., et al. 2006b, ApJ, 640, 854
16. Höflich, P, et al. 1996, ApJ, 459, 307
17. Höflich, P, Wheeler, J.C., & Wang, L. 1999, ApJ, 521, 179
18. Thomas, R.C., et al. 2002, ApJ, 567, 1037
19. Kasen, D., et al. 2004, ApJ, 610, 876
20. Kozma, C., et al. 2005, A&A, 437, 983
21. Sim, S.A. 2007, MNRAS, 375, 154
22. Mazzali, P.A. & Lucy, L.B. 1993, A&A, 279, 447
23. Mazzali, P.A. 2000, A&A, 363, 705
24. Lucy, L. B. 1999, A&A, 345, 211
25. Nakamura, T., et al. 2001, ApJ, 550, 991
26. Maeda, K., et al. 2003, ApJ, 593, 931
27. Kifonidis, K., et al. 2000, ApJ, 531, L123